FRACTURE MECHANICS BEHAVIOUR OF STRESS CORROSION CRACKS

C. Berger[+], G. Mundt*

Stress corrosion cracks may be initiated and grow in certain components during service under corrosive media. Often more than one crack is initiated at the surface. The stress corrosion cracks investigated in the work presented here have an intercrystalline path, are always multiple, branched and have different depths and configurations at different cross sections. Due to the complex crack configuration it is very difficult to calculate the stress intensity factor at the tip of these cracks. Experimental fracture mechanics investigations of such service induced cracks show that their stress intensity factor is 30 to 70 % smaller than the stress intensity calculated for single straight cracks. Theoretical calculations arrive at the same results.

INTRODUCTION

If a stress corrosion crack is found during in-service inspection of an engineering component it is important to predict its subsequent growth rate under service loading conditions and its critical size to unstable propagation. To calculate the critical crack size by fracture mechanics methodology it is essential to know the stress intensity factor of the stress corrosion cracks.

In many cases more than one crack is induced at the surface under corrosive media. In quenched and tempered steels such stress corrosion cracks have an intercrystalline path and are always branched, zig-zag formed and multiple. Their complex configuration needs more clarification to calculate the real stress intensity factor.

The aim of this work is to compare different theoretical examinations of idealized crack configurations with practical investigations of service induced stress corrosion cracks of complex configurations to quantify the stress concentration factor of such different cracks.

+ Kraftwerk Union, Mülheim, Germany
* Kraftwerk Union, Berlin

CRACK CONFIGURATION OF SERVICE INDUCED STRESS CORROSION CRACKS

Metallographic examinations were performed of stress corrosion cracks (SCC) which were, for example, emanating from the key-ways of steam turbine discs due to corrosive environments at high stress concentrations (1-4). The materials are quenched and tempered steels. The cracks have a very complex configuration with regard to number, shape, depth and length. Figures 1 to 3 show such typical SCC. Very often more than one crack is initiated at the surface. In Fig. 1a e.g. four cracks are to be seen, but one of these cracks has no contact to the surface. Sometimes only one or two cracks appear to be nucleated from the surface (Fig. 1f, 2d, 2e). However, parallel metallographic sections always reveal several cracks and crack branches just below. The crack path is always intercrystalline, i.e. along the primary austenitic grain boundaries. Therefore, the orientations of the crack tips have to change at every grain boundary (Fig. 1f, 2d, 2e) and they result in a zig-zag crack path. Also crack branching occurs over more than one grain (Fig. 2c, 2e). Due to this, typical macroscopic crack tip branching is induced (Fig. 1b, 1e, 2, 3). In most cases at least two crack tips occur but sometimes many more crack tips are observed (Fig. 3). Each of these macroscopic cracks have further microscopic crack branching (Fig. 1g, 1h).

Figures 1 and 2 can only show the crack configuration in one specific metallographic section. If one grinds in parallel sections only several tenths of a millimeter below one metallographic section one can find very different configurations of the cracks with regard to numbers, branching and depth of the cracks (Fig. 3). The very complex crack configurations are seen much better in Fig. 1, where the metallographic sections are at a distance up to 25 mm from each other. Stress corrosion sometimes appears to start from a single crack but inevitable such cracks branch to form multiple cracks with very different angles and shapes.

Summarizing these multiple cracks, macroscopic and microscopic crack branching, bending from the straight crack path, different depths and configurations at different cross sections all lead to a very complex crack path which is typical for these stress corrosion cracks.

INFLUENCE OF CRACK CONFIGURATION ON STRESS INTENSITY FACTOR

The value of the stress intensity factor (SIF) for a given loading condition and given crack length is the most important point for a fracture mechanics calculation. Beyond it, the SIF strongly depends on the crack configuration.

A lot of publications about this subject are available today (5-15). They assume crack models for their theoretical as well as for their finite element calculations and also carry out photoelastic examinations to determine the SIF of such crack tips. These calculations of SIF $\underline{k}$ for multiple (a), bent (b, c) and branched (d) cracks are related to single straight (unbranched) cracks $\underline{K}$. The resulting relations k/K are shown in Fig. 4. The different crack models are schematically drawn in the upper part of this diagram.

By more than one parallel orientated crack (a) the k-value at the specific crack tip is reduced by at least 30 % in comparison to a single crack for the considered crack distances. Therefore, the ratio is k/K = 0.7. With more than two cracks, the ratio decreases further, while the outer crack tips (A) have higher k-values than the inner ones (B).

Concerning the determination of SIF of bent (b, c) or branched (d) cracks, the ratio of straight to bent or branched crack length and also the bending angle Θ play an important role. Bending of a crack from a straight orientation, whereby the parts of straight and bent crack lengths are equal, reduces for $\Theta = 30^{\circ}$ the k-value of 20 % to a ratio k/K = 0.8. Under the same conditions an increase of Θ from 30° to 60° leads to k/K = 0.34. In any case an increase of the length of the straight crack path decreases significantly the k/K-ratio.

In the case of a straight crack with one bent crack (c) and $\Theta = 30^{\circ}$ the k/K-ratio from the main crack is about 0.73. In cases of branching in two crack tips (d), the reported results of different authors are in good accordance and lead already for $\Theta = 30^{\circ}$ to k/K-ratios smaller than 0.73. An increase of the branching angles reduces the k-values drastically as well as the number of branches.

Comparing these crack models in Fig. 4 with the metallographically examined SCC (Fig. 1 to 3) a correlation is possible. From there one can establish that also parallel cracks have no straight path due to the intercrystalline crack growth. Therefore, an additional reduction of stress intensity has to be taken into account for this kind of crack path. This is also true for macroscopic branched cracks in addition to microscopic branching with angles larger than 30°. Also very short cracks change their orientation at the first primary austenite grain in a typical branching angle of about 60° (see Fig. 1f, 2d).

Summarizing, one can say that every change of the crack path means a decrease of SIF and leads, for the present SCC configuration models, to k/K-ratios between 0.3 to 0.7. However, these crack configuration models can only consider one specific section and not the strong variations of the crack configurations in different sections. Therefore, these theoretical crack models lead to an overestimation of the real k-value.

EXPERIMENTAL INVESTIGATIONS OF SPECIMENS WITH STRESS CORROSION CRACKS

To establish the influence of service induced stress corrosion cracks on the stress intensity factor, fracture mechanics tests were carried out on specimens with service induced cracks and with cracks initiated in the laboratory under high cycle fatigue conditions.

25 mm thick three point bend specimens with service induced SCC were taken from two turbine discs of 2 % NiCrMo- and 3.5 % NiCrMoV- quenched and tempered steels. In addition to that, specimens of the same material and the same size were precracked according to ASTM E 399 in air as mentioned before.

The fracture mechanics tests were carried out at different temperatures (-196°C, -100°C, -40°C) which guaranteed linear elastic fracture behaviour of the specimens. Therefore, one can state that the constraint of these specimens simulates the stress condition in a large component.

The fracture toughness test results are shown in Fig. 5. The specimens with fatigue precracks (unshaded points) are real K_{Ic}-values with a definite stress intensity factor at the crack tip. For the specimens with service induced cracks a so-called gross SIF at fracture k_{Ic} could be determined with the average crack length of each specimen (shaded points).

The test results of 3.5 % NiCrMoV-steel at -196°C belong to the service induced cracks according to Fig. 2 and fracture surfaces according to Fig. 6. These multiple tests for each condition show that service induced cracks sustain on average 2.5 times and a minimum of 1.75 times larger gross SIF at fracture than the fatigue precracked specimens. The plastic zone sizes at the crack tips of service induced cracks are at maximum load smaller than 0.5 mm so that they do not influence each other. This means that each crack tip leads to a reduction of gross SIF. This does not seem to be always decisive for the specimens tested by Clark (16). Due to the higher plastic deformation at -100°C the plastic zone sizes are larger (about two times) and may influence the reactions at the crack tips. These specimens show on average only a 1.6 times larger gross SIF at fracture than the fatigue precracked specimens.

Further fracture mechanics tests were carried out on 2 % NiCrMo-steel at -100°C and -40°C. Crack configurations and fracture surfaces are according to Fig. 1 and 7. These two tests show that the specimens with stress corrosion cracks sustain 1.5 and 1.8 higher gross SIF k_{Ic} than specimens with fatigue cracks.

The reason for the scatter of test results for comparable specimens is the severe changing of crack configuration along the crack length in one specimen. This is clearly shown by the metallographic (Fig. 1 and 2) and fractographic (Fig. 6 and 7) investigations. The depth and length variations as well as the multiple, zig-zag path and crack tip branching influence the resulting SIF. In addition to that the crack configuration depends on the primary austenite grain size. Because of the intercrystalline crack path, larger grains cause more branching. Furthermore, it is seen from Fig. 6 that parallel initiated cracks at the surface do not always have connections to each other so that a mutual relief of the SIF's takes place.

DISCUSSION

The experimental results can correlate with theoretical calculations. For this the SIF's of specimens with stress corrosion cracks and fatigued cracks are compared at the same loading condition. This comparison is shown in Fig. 4 right. The points are the mean values of each test series and the scattering is the result of a comparison of the lowest K_{Ic}-value with the largest gross SIF k_{Ic} and the largest K_{Ic}-with the lowest k_{Ic}-value respectively.

Considering the total effect of the stress corrosion cracks, they lead to k/K-ratios from 0.3 to 0.7. These experimental results are in good agreement with theoretically calculated k/K-ratios for the observed SCC configuration.

The experimental results as well as the theoretical calculations show that the SIF's of the investigated multiple, bent and branched intercrystalline SCC's are at least 30 % smaller than the factor of a single straight crack of the same size. In a number of experimental investigations with service induced SCC's, even further reductions of the effective SCC's up to 70 % have been actually measured.

This reduction of SIF of SCC in comparison to fatigue cracks means that a component with SCC may be loaded at least 1.4 times higher than a similar component with a single straight (fatigue) crack. Therefore, the critical crack size is at least two times larger than standard fracture mechanics calculations would predict for a single straight crack.

SUMMARY

Service induced stress corrosion cracks in quenched and tempered steels show a complex configuration. They have always an intercrystalline path, are multiple, branched and have different depths, lengths and shapes.

Theoretical investigations concerning simplified models show that multiple, bent and branched cracks such as stress corrosion cracks have stress intensity factors of 30-70 % smaller than single straight cracks of the same size.

Experimental fracture mechanics investigations on different test materials with service induced stress corrosion cracks show at least the same reduction of stress intensity factors.

REFERENCES

1. Engelke W., Jestrich H.A., Schleithoff K., Termuehlen H., American Power Conference, Chicago, Illinois, Apr. 1983.

2. McMinn A. et al., NACE, AIME-ANS-Conf., Myrtle Beach, Aug. 1983.

3. Lyle Jr. F.F., Lamping G.A., ASME/IEEE Power Generating Conf., St. Louis, Missouri, Oct. 1981.

4. Eiselstein L.E., Caligiuri R.D., EPRI Seminar on Low Pressure Turbine Disc Integrity, San Antonio, Texas, Dec. 1983.

5. Klein G., Hodulak L., Z. Werkstofftechn., 9, (1978) 86-92.

6. Isida M., Proc. of the First Int. Conf. on numerical methods in fracture mechanics, Univ. College Swansea, (1978) 81-94.

7. Kitagawa H., Eng. Fracture Mech., 5, (1975) 515-529.

8. Theocaris P.S., J. Mech. Phys. Solids, 20, (1972) 265-279.

9. Theocaris P.S., Eng. Frachture Mech., 17, (1983) 361-366.

10. Lo K.K., J. of Applied Mech., 45, (1978) 797-802.

11. Speidel M.O., NATO Scientific Affairs Division, Brussels, (1971) 345-354.

12. Speidel M.O., EPRI Seminar on Low Pressure Turbine Disc Integrity, San Antonio, Texas, Dec. 1983.

13. Wilson W.K., Cherepko J., Int. J. of Fracture, 22, (1983) 303-315.

14. Vitek V., Int. J. of Fracture, 13, (1977) 481-501.

15. Keller H.P., TÜV-Reports 129 (1981) and 135 (1982), Germany.

16. Clark Jr. W.G., Seth B.B., Shaffer D.H., ASME/IEEE Power Generating Conf., St. Louis, Missouri, Oct. 1981.

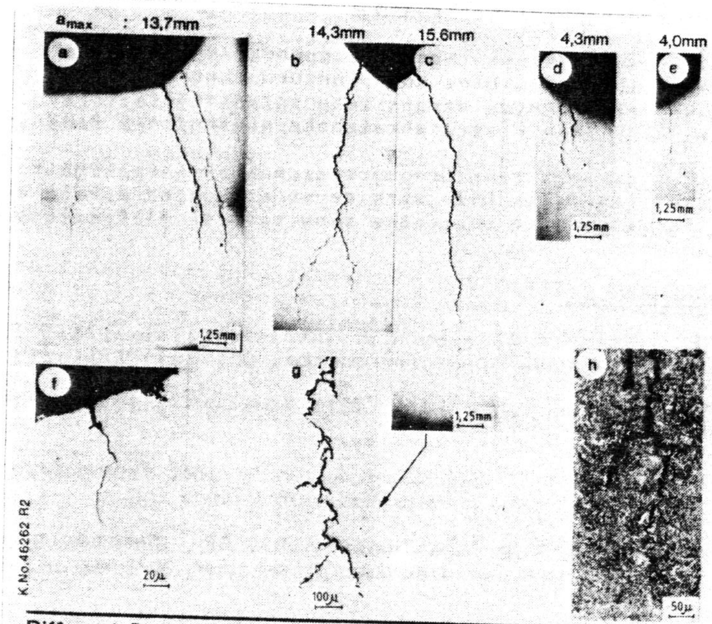

Different Stress Corrosion Crack Configurations
2%NiCrMoV Steel

M84 726

Figure 1

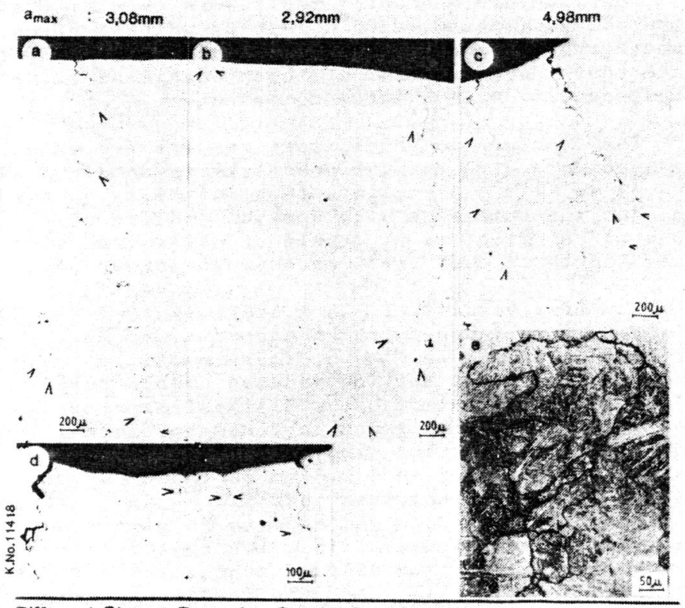

Different Stress Corrosion Crack Configurations
3,5%NiCrMoV- Steel

M84 727

Figure 2

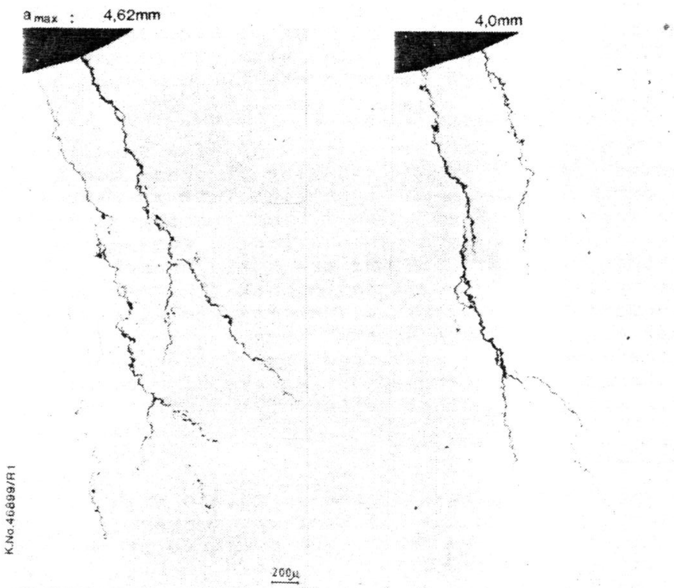

Different Stress Corrosion Crack Configurations
Distance Between Metallographic Sections 1mm

Figure 3

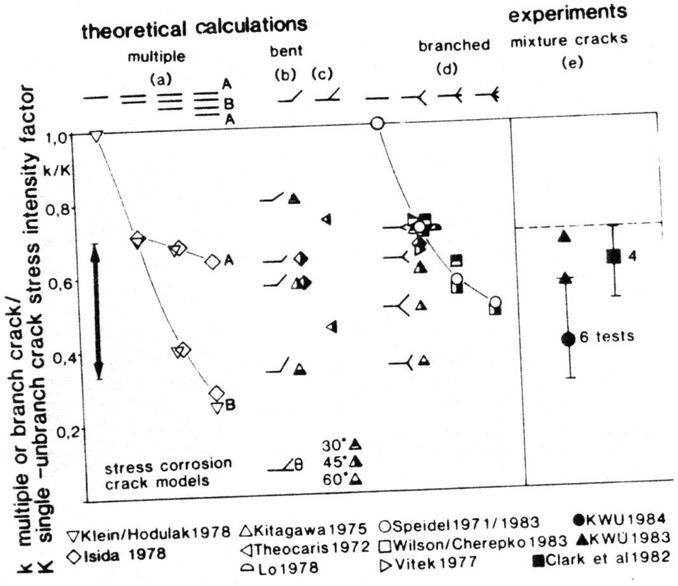

Influence of Crack Configuration on Stress Intensity Factor

M84 732

Figure 4

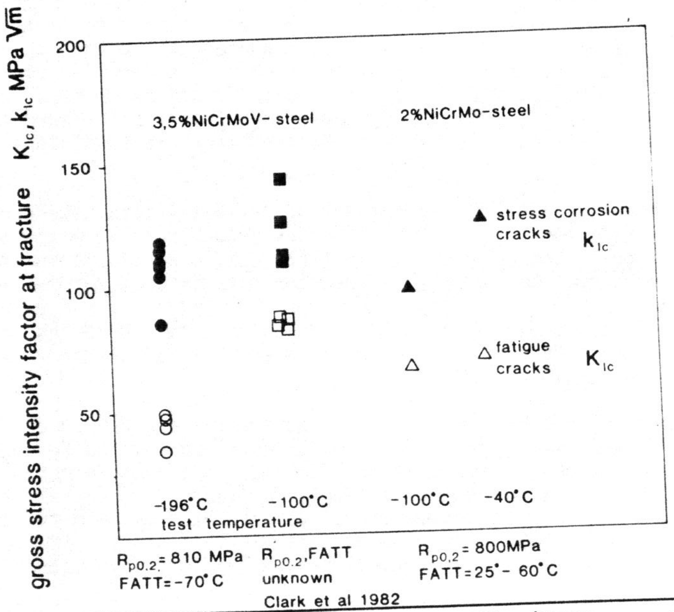

Influence of Crack Configuration on Fracture Toughness

M84 731

Figure 5

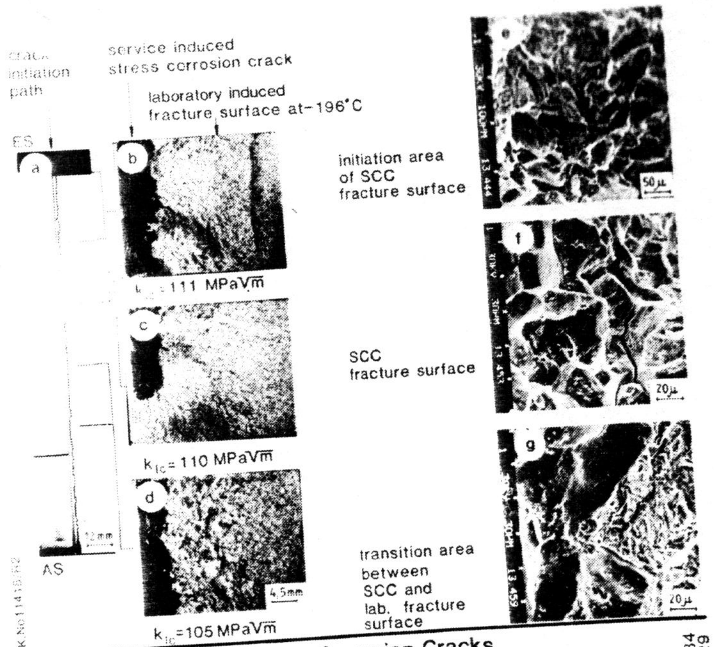

Fracture Surface of Stress Corrosion Cracks
3,5%NiCrMoV Steel

M84 729

Figure 6

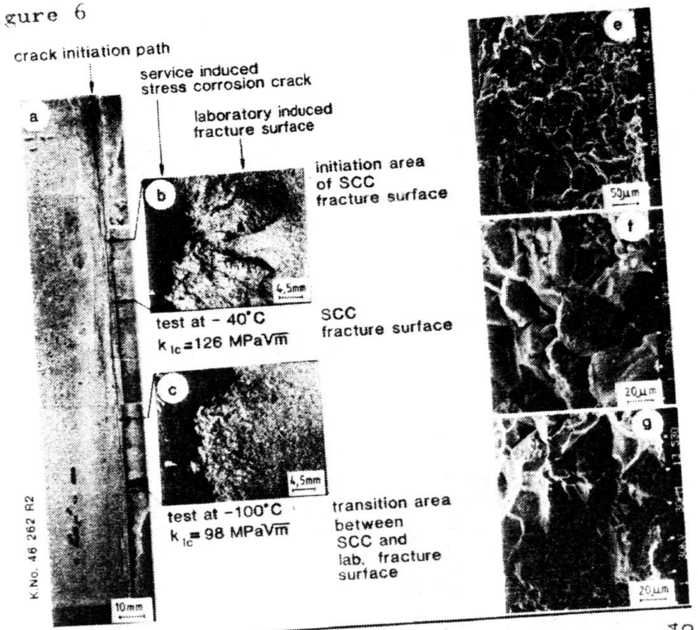

Fracture Surface of Stress Corrosion Cracks
2%NiCrMoV Steel

M84 730

Figure 7